Chemical Science

ROYAL SOCIETY OF CHEMISTRY

EDGE ARTICLE

View Article Online
View Journal | View Issue

Check for updates

Cite this: *Chem. Sci.*, 2020, **11**, 1066

All publication charges for this article have been paid for by the Royal Society of Chemistry

Redox, transmetalation, and stacking properties of tetrathiafulvalene-2,3,6,7-tetrathiolate bridged tin, nickel, and palladium compounds†

Jiaze Xie, Jan-Niklas Boyn, Alexander S. Filatov, Andrew J. McNeece, David A. Mazziotti and John S. Anderson *

Here we report that capping the molecule TTFtt (TTFtt = tetrathiafulvalene-2,3,6,7-tetrathiolate) with dialkyl tin groups enables the isolation of a stable series of redox congeners and facile transmetalation to Ni and Pd. TTFtt has been proposed as an attractive building block for molecular materials for two decades as it combines the redox chemistry of TTF and dithiolene units. $TTFttH_4$, however, is inherently unstable and the incorporation of TTFtt units into complexes or materials typically proceeds through the *in situ* generation of the tetraanion $TTFtt^{4-}$. Capping of $TTFtt^{4-}$ with Bu_2Sn^{2+} units dramatically improves the stability of the TTFtt moiety and furthermore enables the isolation of a redox series where the TTF core carries the formal charges of 0, +1, and +2. All of these redox congeners show efficient and clean transmetalation to Ni and Pd resulting in an analogous series of bimetallic complexes capped by 1,2-bis(diphenylphosphino)ethane (dppe) ligands. Furthermore, by using the same transmetalation method, we synthesized analogous palladium complexes capped by 1,1′-bis(diphenylphosphino)ferrocene (dppf) which had been previously reported. All of these species have been thoroughly characterized through a systematic survey of chemical and electronic properties by techniques including cyclic voltammetry (CV), ultraviolet-visible-near infrared spectroscopy (UV-vis-NIR), electron paramagnetic resonance spectroscopy (EPR), nuclear magnetic resonance spectroscopy (NMR) and X-ray diffraction (XRD). These detailed synthetic and spectroscopic studies highlight important differences between the transmetalation strategy presented here and previously reported synthetic methods for the installation of TTFtt. In addition, the utility of this stabilization strategy can be illustrated by the observation of unusual TTF radical–radical packing in the solid state and dimerization in the solution state. Theoretical calculations based on variational 2-electron reduced density matrix methods have been used to investigate these unusual interactions and illustrate fundamentally different levels of covalency and overlap depending on the orientations of the TTF cores. Taken together, this work demonstrates that tin-capped TTFtt units are ideal reagents for the installation of redox-tunable TTFtt ligands enabling the generation of entirely new geometric and electronic structures.

Received 30th August 2019
Accepted 4th December 2019

DOI: 10.1039/c9sc04381k

rsc.li/chemical-science

Introduction

Conjugated coordination polymers have attracted recent attention due to promising applications in superconductors,[1] energy storage,[2] thermoelectrics,[3] spintronics,[4] and other fields.[5–7] However, delocalized metal–organic systems are still rare and most coordination polymers are limited to architectures constructed with nitrogen and oxygen based ligands.[7,8] Some of the most conductive materials[9] in this area have instead used sulfur based linkers which are perhaps best exemplified by dithiolene units that leverage both a better energy match[10] between sulfur atoms and metal centers and ligand-based redox activity.[4b] Nevertheless, stability and controllable synthetic conditions are still significant challenges associated with the incorporation of dithiolene based linkers. Molecular dithiolene complexes have great utility in addressing these challenges as they allow for a detailed understanding of the properties and reactivity of dithiolene units. Furthermore, molecular dithiolene complexes can be used as transmetalating agents to generate materials in a controlled manner.[5f,10c]

Of possible dithiolene ligands, TTFtt (TTFtt = tetrathiafulvalene-2,3,6,7-tetrathiolate, Fig. 1) is attractive as it combines the above mentioned properties of dithiolenes with the favorable electronic properties of tetrathiafulvalene (TTF).[11] Organic radical salts of TTF and its derivatives are well-known for outstanding electronic properties, such as being

---

Department of Chemistry, The James Franck Institute, University of Chicago, Chicago, Illinois 60637, USA. E-mail: jsanderson@uchicago.edu

† Electronic supplementary information (ESI) available: Experimental details and CIF files. CCDC 1950301–1950306, 1971219, 1971220. For ESI and crystallographic data in CIF or other electronic format see DOI: 10.1039/c9sc04381k

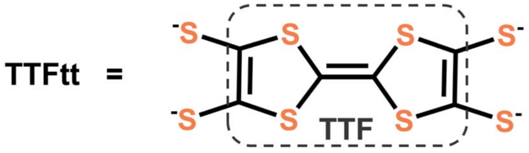

Fig. 1 The structure of TTFtt with the TTF core indicated.

components in organic conductors such as TTF-TCNQ and organic superconductors such as $[\mathrm{TMTSF}]_2[\mathrm{PF}_6]$ (TMTSF: tetramethyl-tetraselenafulvalene).[12] While TTF has been incorporated into coordination polymers to improve conductivity[13] and enable switching of porosity[14] or magnetism,[15] TTFtt has much less precedent in well-defined complexes or materials. Some conductive TTFtt-transition metal chains were reported by IBM Research Laboratory in 1979 with limited characterization data.[16a] In 1995, McCullough and coworkers crystalized the first homobimetallic TTFtt complex and the TTFtt unit was proposed as a promising building block for new magnetic, electronic and optical materials.[17a,b] However, there has been little progress towards this end over the following decades. Only one report of installing TTFtt between fullerene supported Co centers using a decarbonylative process at high temperature has been structurally characterized and limited characterization has been reported on molybdocene fragments bridged by TTFtt.[18]

The primary challenge with the incorporation of TTFtt into molecules or materials is the sensitivity of this moiety and its synthons. Unprotected $\mathrm{TTFttH_4}$ has not been isolated and characterized, although $\mathrm{TTFttLi_4}$ can be generated transiently as a highly reactive and sensitive solid for metalations as reported in McCullough's work.[17] The conventional synthetic technique for the incorporation of TTFtt involves the *in situ* deprotection of derivatives such as 2,3,6,7-tetrakis(2′-cyanoethylthio)tetrathiafulvalene, $\mathrm{TTFtt(C_2H_4CN)_4}$.[19] This deprotection typically requires the use of an excess of strong base which limits the choice of solvent and also leads to undesirable side reactions due to the highly basic, nucleophilic, and reducing properties of the $\mathrm{TTFtt^{4-}}$ tetraanion. Furthermore, the required excess base may also introduce side-reactions. These issues have directly limited the investigation and incorporation of TTFtt.

To alleviate these issues and enable the facile and controlled installation of TTFtt between transition metals, we were inspired by previous work by Donahue and coworkers that demonstrated that capping of dithiolene units such as 1,2,4,5-benzenetetrathiolate with dialkyltin groups enables smooth transmetalation to transition metals.[20,21] In the current work, we successfully employ a similar strategy to stabilize the TTFtt unit and isolate the stable and soluble bis-dibutylstannylated complex $\mathrm{TTFtt(SnBu_2)_2}$, **1**. Furthermore, and distinctly from other dithiolene tin agents, complex **1** is redox-active and can be sequentially oxidized to generate stable cation radical and dicationic TTF cores in the isolable complexes $[\mathrm{TTFtt(SnBu_2)_2}][\mathrm{BAr^F_4}]$, **2** and $[\mathrm{TTFtt(SnBu_2)_2}][\mathrm{BAr^F_4}]_2$, **3** ($[\mathrm{BAr^F_4}]$ = tetrakis(3,5-bis(trifluoromethyl)phenyl)borate). Compounds **1–3** are efficient transmetalating agents to generate $\mathrm{(dppeNi)_2TTFtt}$, $[\mathrm{(dppeNi)_2TTFtt}][\mathrm{BAr^F_4}]$ and $[\mathrm{(dppeNi)_2TTFtt}][\mathrm{BAr^F_4}]_2$ (dppe = 1,2-bis(diphenylphosphino)ethane, **4–6**). To demonstrate the generality of transmetalation with tin precursors to other transition metals, we also prepared the Pd complexes, $\mathrm{(dppePd)_2TTFtt}$, $[\mathrm{(dppePd)_2TTFtt}][\mathrm{BAr^F_4}]$, $\mathrm{(dppfPd)_2TTFtt}$ and $[\mathrm{(dppfPd)_2TTFtt}][\mathrm{BAr^F_4}]$ (dppf = 1,1′-bis(diphenylphosphino)ferrocene, **7–10**). Crystallographic analyses of these materials reveal a variety of stacking arrangements of the TTF cores. Application of cutting-edge variational 2-electron reduced density matrix theory elucidates how the twisting of the TTF–TTF cores affects their electronic structure, a feature which is critical to understand their long-range transport properties. In sum, this work demonstrates that capping TTFtt with dialkyl tin units enables the stabilization and isolation of an unusual redox series of the TTFtt ligand and facile installation of all of these redox congeners onto transition metals. This work now allows for the formation of new materials featuring TTFtt with precise control over synthetic conditions and redox state.

Results and discussion

Synthesis of Sn and Ni capped TTFtt redox congeners

All of the reactions involved with Sn and Ni complexes are summarized in Scheme 1. Compound **1** was synthesized *via* deprotection of $\mathrm{TTFtt(C_2H_4CN)_4}$ with excess sodium methoxide and subsequent reaction with excess $\mathrm{Bu_2SnCl_2}$ in MeOH. In contrast to the high reactivity of the $\mathrm{TTFtt^{4-}}$ tetraanion, **1** was indefinitely stable as a solid at room temperature and red crystals can be obtained *via* recrystallization from boiling acetonitrile at 80 °C. The stability of **1** under these conditions suggests that the use of common solvothermal synthetic conditions for coordination polymers should be viable. The cyclic voltammogram (CV) of neutral **1** shows two quasi-reversible features, suggesting that two oxidized species are chemically accessible (Fig. 2A). The reagents $[\mathrm{Fc}][\mathrm{BAr^F_4}]$ and $[\mathrm{Fc^{BzO}}][\mathrm{BAr^F_4}]$ ($\mathrm{Fc^+}$ = ferrocenium, $\mathrm{Fc^{BzO}}$ = benzoyl ferrocenium) were therefore used to chemically access the singly and doubly oxidized redox congeners **2** and **3**. While brown crystals of **2** were obtained which verified the proposed structure of this compound, the oxidation reaction of **1** with 2 equivalents of $[\mathrm{Fc^{BzO}}][\mathrm{BAr^F_4}]$ under the same conditions led to the formation of $\mathbf{3}\cdot 2\mathrm{Fc^{BzO}}$ where each Sn center is coordinated by an additional $\mathrm{Fc^{BzO}}$ molecule (Fig. S53†). To avoid the formation of these adducts, the reaction and crystallization were both conducted in THF solvent which enabled the isolation of green crystals of $\mathbf{3}\cdot 2\mathrm{THF}$.

The ability of these stannylated species for ligand transmetalation was tested by reactions with 2 equivalents of $\mathrm{dppeNiCl_2}$ in DCM or $\mathrm{Et_2O}$ at room temperature. All metalation processes proceed smoothly and provide the three corresponding dinickel complexes, **4–6**, in good yield. Complex **4** with a formally neutral TTF core was obtained as an insoluble orange-yellow powder. Compounds **5** and **6**, however, were much more soluble enabling crystallization as dark brown and purple crystals respectively. The Ni complexes are also redox-active as indicated by their CV's which show two quasi-reversible oxidations shifted ~0.4 V more negative than those

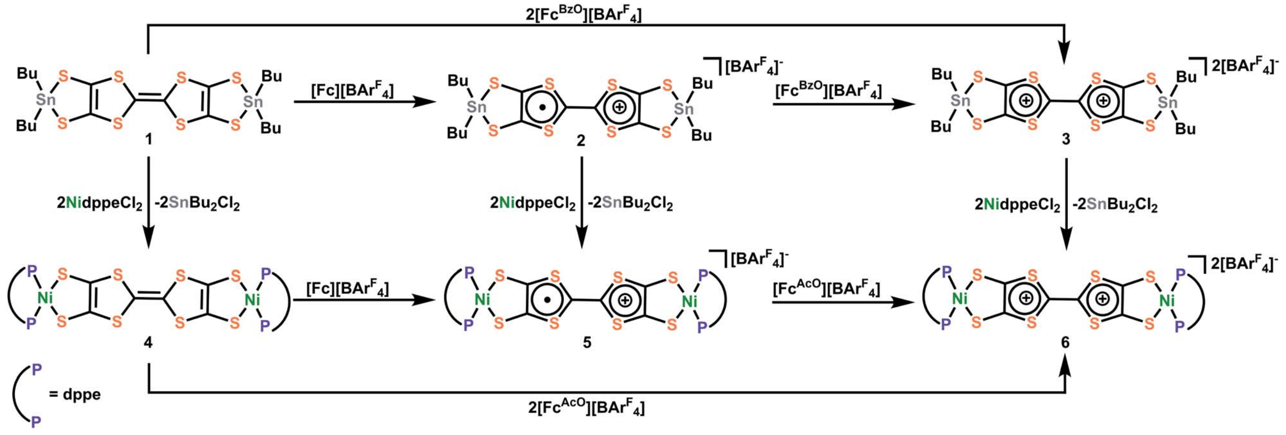

Scheme 1 The synthesis of Sn and Ni complexes with TTFtt as a bridging ligand.

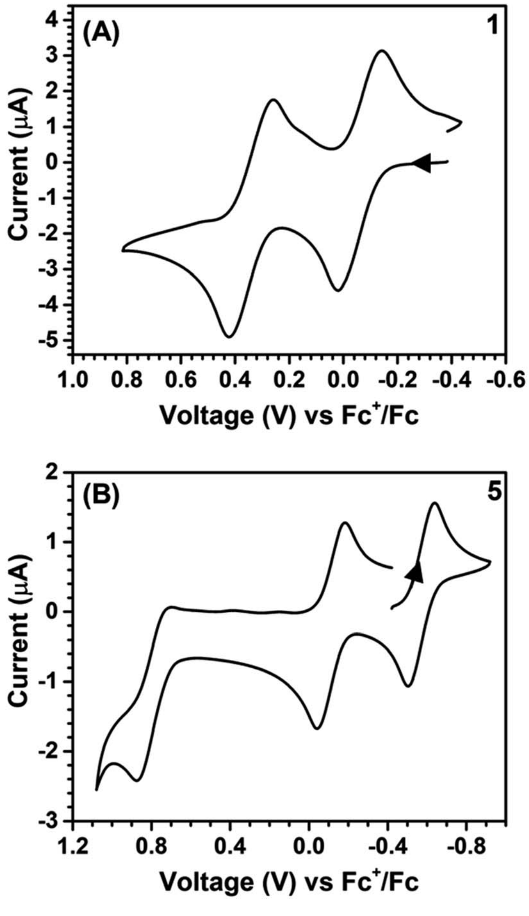

Fig. 2 Cyclic voltammograms of 1 (A) and 5 (B). Arrow denotes scan direction. Conditions: DCM, 0.1 M [TBA][PF$_6$], 0.1 V s^{-1}.

observed in **1** (Fig. 2B). Compounds **5** and **6** could also be generated by oxidizing **4** with $[\mathrm{Fc}][\mathrm{BAr}^{\mathrm{F}}_4]$ and $[\mathrm{Fc}^{\mathrm{AcO}}][\mathrm{BAr}^{\mathrm{F}}_4]$ ($\mathrm{Fc}^{\mathrm{AcO}}$ = acetyl ferrocenium) respectively as verified by NMR spectroscopy.

These compounds demonstrate that the stannylation of the reactive and unstable TTFtt^{4-} anion is an effective strategy to both stabilize unusual redox series as well as to enable facile transmetalation to transition metals. These tin agents are much more stable than conventional *in situ* formed TTFtt^{4-} anions, allowing for purification, long-term storage, and convenient utility under a wide range of conditions with various solvents. In addition to these advantages, complexes **2** and **3** provide additional synthetic flexibility *via* controlled redox "doping." For instance, complex **2**, with a TTF radical cation core, enables direct insertion of radical linkers between metal centers. Furthermore, **3** is one of only a few examples of isolable dicationic TTF motifs.[22,23] The facile redox and transmetalation chemistry of **1–3** paves the way for the synthesis of new materials with precisely tuned redox states.

Solid state structures

Compounds **1–3**, **5**, and **6** have been crystallographically characterized and their single crystal X-ray diffraction (SXRD) structures are shown in Fig. 3. Their packing patterns are shown in Fig. S48–S52.† Compounds **1**, **3**, and **5** crystallize in the triclinic space group $P\bar{1}$, compounds **2** and **6** crystallize in the monoclinic space groups $P2_1/c$ and $C2/c$, respectively. The geometrical parameters of the TTF cores such as bond lengths and dihedral angles are typically sensitive to the redox state of the TTF unit.[22f] Interestingly, in the present Sn capped redox series some of these changes are muted. For instance, planarization of the TTF core is typically observed only upon oxidation, but in **1** the neutral TTF rings are nearly coplanar (Fig. S46†). The trends in the C–C and C–S bond lengths are more informative and are shown in Table 1. As the molecular charge increases, the C–C bond distances in the TTF cores also increase, while the C–S bond lengths generally decrease. These trends are consistent for both the Sn series in **1–3** and the Ni series from **5** to **6**. These changes are consistent with previous studies showing similar geometric trends upon oxidation of TTF molecules.[22f] Conversely, there is little change or trend in the M–S distances for either the Sn or the Ni complexes, supporting the assignment of primarily TTF-centered redox events.

Most of these compounds also display intermolecular TTF–TTF packing interactions in their SXRD structures, as has been

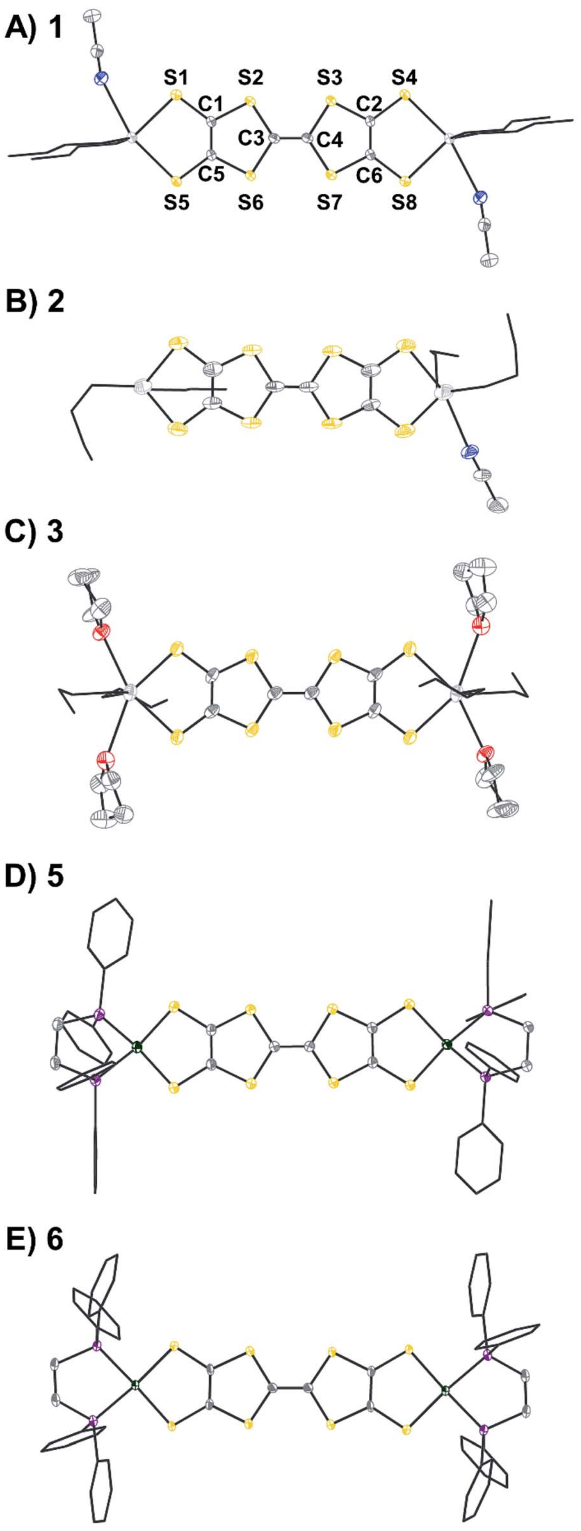

Fig. 3 Single crystal X-ray diffraction (SXRD) structures of (A) **1**·2MeCN, (B) **2**·0.5THF·0.5MeCN, (C) **3**·4THF, (D) **5**, and (E) **6**·[BAr$^{\mathrm{F}}_4$] anions, solvent, H atoms, and disorder are omitted and *n*-butyl and phenyl groups are shown in wireframe for clarity. The labeling scheme shown for **1** applies for all compounds. Ellipsoids are shown at 50% probability. Selected bond lengths are included in Table 1. Sn is shown in light grey; Ni, green; S, yellow; P, purple; O, red; N, blue; C, dark grey.

observed extensively in other TTF based systems.[12] Compounds **1**, **5** and **6** show extended one dimensional chains *via* weak side-to-side sulfur–sulfur interactions, although another unusual additional polymorph of **5** was found which will be discussed more thoroughly below. Compound **2** forms dimers in the solid-state *via* π-stacking. Finally, dicationic **3** shows no significant intermolecular interaction as the TTF core is effectively shielded by the large [BAr$^{\mathrm{F}}_4$] anions.

Electronic properties of Sn and Ni complexes

The synthetic ease of accessing these series of redox congeners motivates examination of their electronic structure. As discussed above, CV shows two oxidation peaks for **1** at −0.14 V and 0.28 V *vs.* Fc$^+$/Fc. In **5** these features shift to −0.58 V and −0.11 V respectively. The Ni species display an additional irreversible peak at 0.79 V *vs.* Fc$^+$/Fc which is tentatively assigned as a Ni$^{\mathrm{II}}$ to Ni$^{\mathrm{III}}$ oxidation. Redox events at similar potentials were seen for the preliminary study of the complex (dpppNi)$_2$TTFtt (dppp = 1,3-bis(diphenylphosphino)propane) although limited characterization of this complex is reported.[17c,d] It is worth noting that appreciable film deposition at the working electrode surface was observed on repeated scans in our CV studies. We anticipate that this arises from reaction of the oxidized congeners with the [PF$_6$]$^-$ electrolyte anions as has been previously proposed.[21b] The CV of **5** with [Na][BAr$^{\mathrm{F}}_4$] as the electrolyte medium was performed and no obvious degradation was observed over multiple scans. This enhanced stability from fluorinated aryl borates is also reflected in the synthetic chemistry mentioned above. The lack of oxidative features between 0 and 0.6 V suggests that the dicationic species **6** is potentially air-stable. To test this possibility, a CDCl$_3$ solution of **6** was exposed to air for 12 hours and then analyzed by NMR spectroscopy. Comparison of the ^{1}H and ^{31}P NMR spectra before and after this exposure indicate nearly no decomposition with the exception of a very small amount of oxidized phosphine (<2%, Fig. S23 and S24†). While crude, this initial test indicates that materials composed of typically air-sensitive TTFtt synthons may be made air-stable by tuning the charge state of the TTF core.

In order to more firmly assign the redox features observed by CV, UV-vis-NIR investigations were carried out on the Sn compounds **1–3** and on the soluble Ni complexes **5** and **6** (Fig. 4). Compound **1** has an intense feature at 328 nm, assigned as arising mainly from π–π* transitions.[24] Upon oxidation to **2** a broad feature emerges at 1053 nm. Appearance of this new low-energy absorption band has been previously interpreted as arising from the formation of π-dimers.[25] This absorption band blue-shifts to 941 nm upon further oxidation. Similar spectral features are observed in the Ni complexes **5** and **6** (Fig. 4b). Compared to **2** and **3**, the NIR absorption features of **5** and **6** both show a distinct red-shift (Fig. S42 and S43†).

In addition to UV-vis-NIR spectra, the signals of the TTF radicals were investigated by EPR spectroscopy. The EPR spectrum of **2** in THF (Fig. S25†) shows an isotropic feature at g = 2.008, consistent with an organic radical. Conversely, anisotropic signals at g = 2.013, 2.007, and 2.003, were observed in the EPR

Table 1 SXRD metrical parameters for **1–3**, **5**, and **6**

	C_3–C_4 (Å)	$C_{1,2}$–$C_{5,6}$ (Å)	C–S^a (Å)	M–S (Å)	M–S′ (Å)
1	1.333(5)	1.338(4)	1.746(3)–1.760(3)	2.4579(7)	2.5050(7)
2^b	1.351(16)	1.37(2)	1.72(1)–1.76(1)	2.455(4)	2.446(3)–2.563(3)
3	1.436(18)	1.402(12)	1.681(9)–1.732(8)	2.535(2)	2.502(3)
5	1.385(2)	1.361(2)	1.726(2)–1.740(1)	2.1616(5)	2.1750(8)
6	1.412(5)	1.379(3)	1.704(2)–1.726(2)	2.1684(7)	2.1790(7)

^{a} C–S bonds includes all C–S bonds in the TTFtt linker. ^{b} The two five-membered rings of **2**'s TTF core are not symmetric.

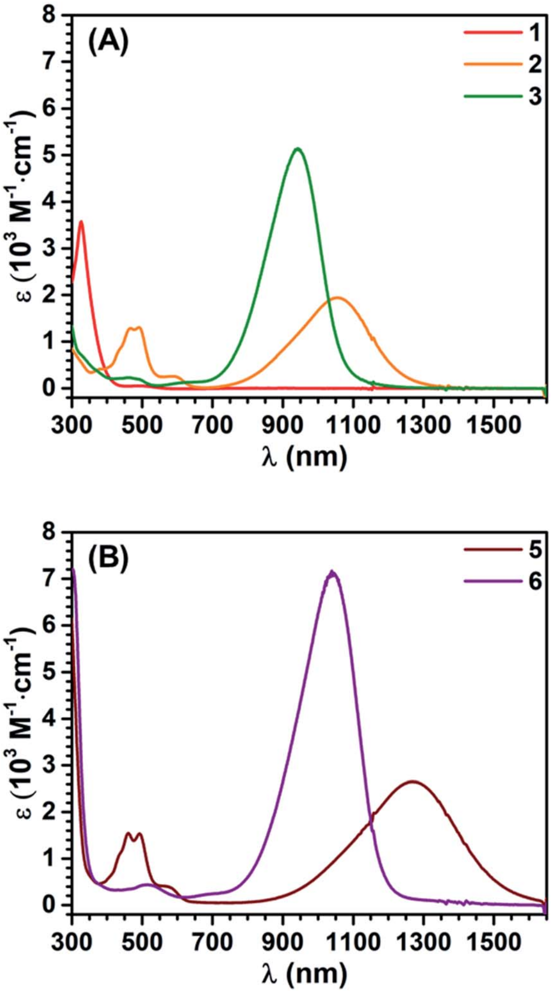

Fig. 4 UV-vis-NIR absorption spectra of **1–3** (A), **5** and **6** (B) in DCM. Concentration: **1**, 92 μM; **2**, **3**, **5** and **6**, 50 μM.

spectrum of **5** (Fig. S26†). Similarly, anisotropic signals have been observed in other TTF radical systems.[26] The spectroscopic and structural data for these compounds is very similar to that observed for other TTF systems again suggesting that the redox events of TTFtt are largely localized on the TTF core.

Transmetalation to Pd

To further demonstrate the versatility and generality of transmetalation with these tin precursors to other transition metals, we prepared the Pd complexes, $(\mathrm{dppePd})_2$TTFtt, $[(\mathrm{dppePd})_2\mathrm{TTFtt}][\mathrm{BAr}^{\mathrm{F}}_4]$, $(\mathrm{dppfPd})_2$TTFtt and $[(\mathrm{dppfPd})_2\mathrm{TTFtt}][\mathrm{BAr}^{\mathrm{F}}_4]$ (**7–10**; dppf = 1,1′-bis(diphenylphosphino)ferrocene) (Scheme 2). Analogously to the Ni examples above, mixing $\mathrm{dppePdCl}_2$ or $\mathrm{dppfPdCl}_2$ with complexes **1** and **2** results in the new bridged Pd congeners. Complexes **7** and **9** which contain neutral TTF cores were isolated as insoluble pink/orange powders, while complexes **8** and **10** were crystalized as dark brown needles and were characterized by SXRD analysis (Fig. S54 and S55†). The radical species **8** and **10** possess similar geometric parameters, UV-vis-NIR features (Fig. S44†), and EPR signals (Fig. S27 and S28†) to compound **5**.

Both sets of Pd complexes are also redox-active. As the CV of **10** shows (Fig. S41†), two quasi-reversible peaks assigned to oxidation of the TTF core are observed below 0 V (−0.53 and −0.08 V *vs.* $\mathrm{Fc}^+/\mathrm{Fc}$). Three additional quasi-reversible features are also observed at 0.72, 0.94 and 1.26 V and are attributed to a two-electron oxidation of both ferrocene units from dppf and two separate one-electron $[\mathrm{Pd\text{-}dithiolene}]^{0/1+}$ processes by comparison to the CV spectrum of (dppfPd)dmit (dmit = 1,3-dithiole-2-thione-4,5-dithiolate).[27] Complex **8** shows similar but more negative redox features without the additional ferrocene oxidations (Fig. S40†).

The synthesis of $(\mathrm{dppfPd})_2$TTFtt has previously been reported by using *in situ* formed TTFtt anions.[28] The material from this previous report did not show any redox peaks in its CV with a glassy-carbon electrode. When using a Pt-button working electrode, only three features were found at −0.05, 0.42 and 0.90 V *vs.* $\mathrm{Ag}/\mathrm{Ag}^+$ assigned as the oxidations of the ferrocene units (−0.05) and TTF core (0.42 and 0.90). Our CV experiment was performed on crystalline **10**, whose composition and structure are firmly confirmed by a variety of techniques including SXRD. Furthermore, the redox behaviour of **10** is consistent with the redox behaviour of complexes **5** and **8**. We also note that the color and solubility of $(\mathrm{dppfPd})_2$TTFtt from the previous literature report is quite different than what we have observed for this complex.

These results raise questions about the previous report of the preparation of $(\mathrm{dppfPd})_2$TTFtt with *in situ* formed TTFtt^{4-}. To address these inconsistencies, we repeated the synthesis of $(\mathrm{dppfPd})_2$TTFtt following the previously reported procedure three times and consistently obtained low yields of 10% or less (*versus* 66% reported). The small amount of collected product prevented us from detailed characterization of this material. Taken all together, the direct comparison with previous preparations of $(\mathrm{dppfPd})_2$TTFtt prepared through the conventional method highlights the versatility and efficiency of the TTFtt-tin

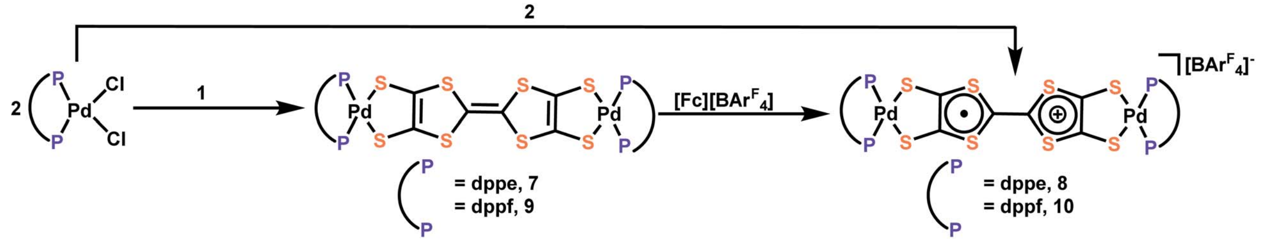

Scheme 2 The synthesis of Pd complexes with TTFtt as a bridging ligand.

precursors we report here. This new synthetic protocol enables isolation of new pure complexes and may challenge previous preparations and assignments of these species that suffer from the *in situ* generation of TTFtt^{4-}.

Packing and dimerization of TTFtt units

Although the NIR absorptions for radical cations and dications may indicate the presence of π-dimer formation in solution, this interpretation has been questioned.[29] To probe the possibility of dimerization in solution, room temperature Evans method experiments on $CDCl_3$ solutions of **5** were performed. The experimentally measured magnetic moment $\mu_{\text{eff}} = 1.19$ BM is smaller than the predicted spin-only value of 1.73 BM suggesting that some degree of oligomerization is occurring. Additionally, spin quantitation of the EPR spectrum of **5** at 15 K indicates <10% of the expected signal based on the concentration of **5**, also supporting some degree of dimerization. Variable-temperature UV-vis-NIR spectroscopic experiments (Fig. S45†) indicate an increase of the absorption peak in the NIR region with cooling, suggesting that the equilibrium shifts to oligomerization as the temperature decreases.[29]

In addition to these solution studies, we were also interested in examining the effect of the solid-state packing of these molecules. As mentioned, solid-state packing of TTF cores is well-known, and much of the bulk transport properties of TTF based systems arises from their π–π and sulfur–sulfur interactions in the solid state, particularly in single component conductors.[11–13,30] The packing of these compounds has been discussed above and is largely similar to previously reported systems. Solid state magnetic measurements were performed on **5** and indicate a diamagnetic compound, which is also similar to previously reported radical cations of TTF.[18b,31]

During the course of these studies, however, we isolated a poorly diffracting alternative polymorph of **5**. While the poor quality of this crystal prevented a full structural solution, we have been able to obtain sufficient resolution to observe a stacking interaction which has a twist of the TTF cores by a nearly orthogonal ∼90° (Fig. 5). TTF stacking most commonly has a parallel arrangement, although there are examples of similar twisted interactions, particularly when supported by auxiliary polymeric superstructures.[13] This structure of **5** is somewhat unusual in that the rotated 1D column of **5** is composed of two elements: trimers with asymmetric orthogonally crossed interactions and dimers with more typical parallel interactions (Fig. 5, and S56–S58†). Higher-quality crystals of complex **8** were obtained and the structure of this species displays very similar chains (Fig. S54†), verifying this unusual structural motif. The strength of TTF–TTF interactions and overlap is dependent on S–S interactions between TTF cores. In these unusual stacks however, the orthogonal and parallel interactions may lead to different overlaps which prompted us to investigate what additional effect the twisting of the TTF–TTF cores has on their interaction.

Computational analysis of TTFtt–TTFtt interactions

We then undertook calculations on **5** as a model for the effect of the twisted TTF–TTF interactions. Understanding the

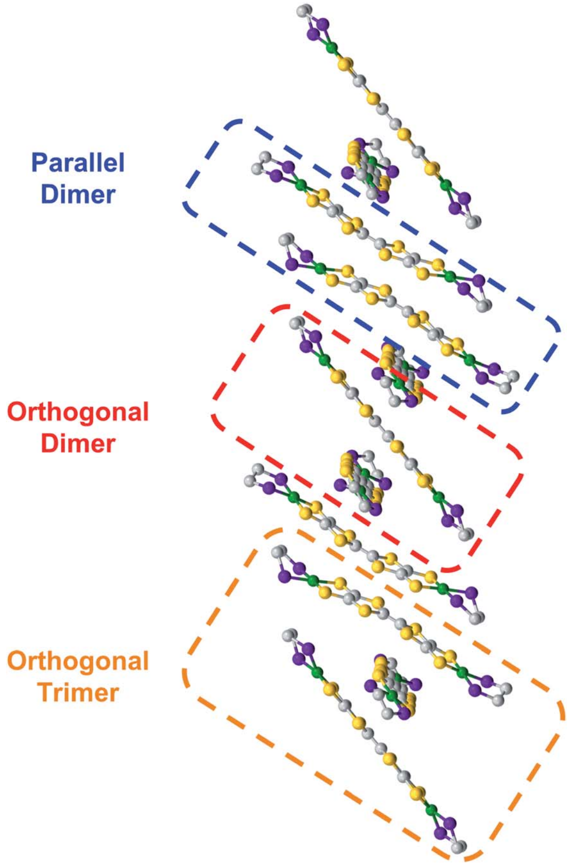

Fig. 5 Stacking diagram for twisted polymorph of **5** with phenyl groups, hydrogen atoms, and anions removed for clarity. Ni is shown in green, S in yellow, P in purple, and C in grey. The computationally examined parallel dimer, orthogonal dimer, and orthogonal trimer are indicated.

interactions in the dimer and trimer units in detail and how the twisting of the TTF–TTF interaction affects electronic structure requires large scale CASSCF calculations with extensive active spaces, leading to prohibitively high computational costs with conventional methods. Instead, we employed variational 2-electron reduced density matrix (V2RDM) techniques,[32] which have previously been demonstrated to successfully describe the electronic structure of a variety of strongly correlated large molecules.[33] V2RDM calculations were carried out as implemented in the Maple Quantum Chemistry Package.[34] The phenyl ligands were replaced with methyl groups and [18,20] active space V2RDM calculations with the 3-21G basis set were performed for both geometries providing the data shown in Table S7.†[35] The electronic structures of both arrangements show significant degrees of correlation as demonstrated by partial occupancies in their frontier natural orbitals (NOs). The orthogonal arrangement shows more radical character, with frontier orbital natural occupation numbers (NON) of 1.224860 and 0.771141 suggesting significant bi-radical character, compared to 1.49923 and 0.51331 in the parallel arrangement. Mulliken charges show an effective charge of +1/2 for the Ni centers in both geometries, with a slightly higher cumulative charge of 1.94745 in the parallel arrangement compared to 1.70585 in the orthogonal system.

Frontier orbital densities, occupations and splittings for the parallel dimer and orthogonal dimer and trimer are shown diagrammatically in Fig. 6A and B respectively. All frontier NOs are localized on the bridging ligand with no involvement of the Ni centers, consistent with experimental results. There are significant differences in the orbital configurations elucidating the variation in frontier NON across the two arrangements. The larger splitting of the NO occupancy in the parallel arrangement clearly arises from better orbital overlap between the two monomers, allowing for greater energetic orbital splitting into NO 384 with significant antibonding character, showing no overlap between the two monomers, and NON 383 with significant bonding character and orbital overlap. In contrast, the orthogonal dimer shows two frontier NOs with very similar densities, both showing significant bonding character and overlap between the two monomers, yielding a smaller splitting and correspondingly greater bi-radical character.

As the orthogonal dimeric arrangement is actually part of a larger asymmetrically stacked unit, a trimeric unit was run separately in V2RDM using a [17,20] active space and the 3-21G basis set, giving a SCF calculation with 1308 orbitals. Data are shown in Table S8.† Similar to the dimeric case, the trimer unit exhibits clear radical character and three partially occupied NOs with NON of 1.32748, 0.97218 and 0.64935. Mulliken charges in this arrangement are particularly symmetric with each nickel showing a charge of 0.43 to 0.45 with very little variation between the individual centers. Transitioning from a dimeric to a trimeric unit gives rise to splittings and symmetries in line with a classic Hückel picture with the orbitals splitting into bonding, non-bonding and antibonding. The bonding and antibonding orbitals NO 574 and 576 both show roughly equal distribution of the electron density across all three units within the trimer. NO 574 has good matching of the phases between the orbitals localized on each of the units in the trimer leading to overlap between the orbitals on all units and giving rise to significant bonding character and a NO occupancy of 1.32748. Constituent orbitals of NO 576 in contrast constitute a worse matching of the phases, reducing overlap between the

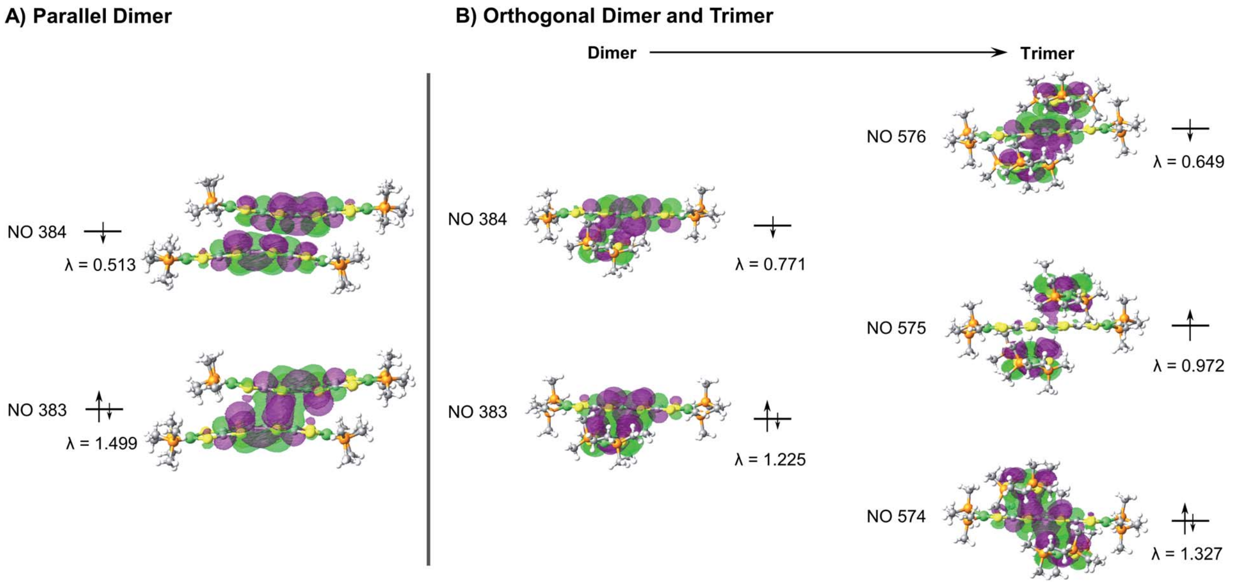

Fig. 6 Frontier NO occupations and densities for (A) the parallel dimer, showing the splitting into bonding and antibonding orbitals. Data and densities obtained *via* [18,20] V2RDM calculations with a 3-21G basis set. (B) For the orthogonal dimer and trimer. Good overlap and correspondingly small splitting in the orthogonal dimer give way to a clear splitting into bonding, non-bonding and antibonding frontier NOs upon transitioning to the orthogonal trimer. Data and densities obtained *via* V2RDM calculations with a 3-21G basis set and [18,20] and [17,20] active spaces for the dimer and trimer respectively.

individual units and leading to an overall antibonding interaction and a NO occupancy of 0.64935. Singly occupied nonbonding NO 575 is localized on the top and bottom molecules with a nodal plane and negligible density on the central unit, leading to an electron entangled across the two isolated top and bottom units within the trimer.

The results from V2RDM CASSCF calculations help rationalize the appearance and stability of the different morphologies in the TTFtt stacks. Packing geometries in both the parallel and orthogonal arrangement allow for good orbital overlap between the individual units. Both morphologies show the frontier natural orbitals form *via* π–π stacking utilizing orbitals localized on the TTF linkers. The resulting NOs differ slightly between the different morphologies with overlap in the parallel geometry allowing for better splitting into clear bonding and antibonding frontier orbital pairs, reducing radical character. The splitting is less pronounced in the orthogonal dimer; however, as the chain size increases clear splitting into bonding, non-bonding and antibonding frontier orbital pairs is recovered in the trimer. In all cases partial occupations in the frontier NOs is retained, allowing for radical chain development and electron entanglement across multiple units.

In 1985, Hoffman and coworkers predicted possible stacking structures of metal bisdithiolenes based on qualitative molecular orbital and band structure calculations.[36] Soon afterwards, in 1988, a LAXS (Large Angle X-ray Scattering) and EXAFS (Extended X-ray Absorption Fine Structure) investigation was performed on amorphous nickel tetrathiolate polymers, proposing two types of polymers with hexagonal (honeycomb) and tetragonal packings for small and large cations, respectively.[37] However, the stackings of the TTFtt radicals in **5** and **8** highlight the key role of strong intermolecular interactions between radicals in the control of morphology. In sum, the stabilization and synthetic access provided by the Sn capped compounds reported here enables the observation of a variety of solid-state interactions of the TTF core. We anticipate that the redox flexibility of these synthons will enable the observation of novel interactions and electronic structures in TTFtt based coordination polymers.

Conclusions

TTFtt is an attractive building block for redox-switchable and highly conjugated metal–organic materials. The work presented here demonstrates that capping TTFtt with dialkyl Sn groups stabilizes this ligand and facilitates the use of redox-active TTFtt moieties. Furthermore, the redox flexibility of these synthons helps to precisely control doping, charge, and crystallinity *via* homogeneous molecular reactions. The synthesis and characterization of the corresponding dinickel and dipalladium complexes validates the ease of transmetalation as a synthetic strategy. We have also observed an unusual "twisted" geometry in the solid state which impacts the electronic structure of the TTF–TTF interaction, effectively demonstrating the utility of these new synthons. Overall, this work demonstrates the usefulness of molecular TTFtt compounds and offers exciting promise for the design and synthesis of multi-functional TTFtt-based coordination polymers.

Conflicts of interest

There are no conflicts to declare.

Acknowledgements

We thank Prof. Jing-lin Zuo for the gift of an initial TTFttPG sample. We thank Dr Ethan Hill for assistance with EPR spectroscopy and Kate Jesse for the assistance with UV-vis-NIR spectroscopy. Parts of this work were carried out at the Soft Matter Characterization Facility of the University of Chicago. J. S. A. and D. A. M. gratefully acknowledge support for this work from the U. S. Department of Energy, Office of Science, Office of Basic Energy Sciences, under Award No. DE-SC0019215. D. A. M. gratefully acknowledges the National Science Foundation (NSF) Grant No. CHE-1152425, and the United States Army Research Office (ARO) Grant No. W911NF-16-1-0152. This work was supported by the Chicago MRSEC, which is funded by NSF through Grant DMR-1420709. The University of Chicago is thanked for startup funds. Use of the Advanced Photon Source at Argonne National Laboratory was supported by the U. S. Department of Energy, Office of Science, Office of Basic Energy Sciences, under Contract No. DE-AC02-06CH11357, and we thank Dr Yu-Sheng Chen for assistance with SXRD data acquisition at beamline 15-ID-B, C, and D.

Notes and references

1 X. Huang, S. Zhang, L. Liu, L. Yu, G. Chen, W. Xu and D. Zhu, Superconductivity in a Copper(II)-Based Coordination Polymer with Perfect Kagome Structure, *Angew. Chem., Int. Ed.*, 2018, **57**(1), 146–150.

2 (*a*) L. Wang, Y. Han, X. Feng, J. Zhou, P. Qi and B. Wang, Metal–Organic Frameworks for Energy Storage: Batteries and Supercapacitors, *Coord. Chem. Rev.*, 2016, **307**, 361–381; (*b*) D. Sheberla, J. C. Bachman, J. S. Elias, C.-J. Sun, Y. Shao-Horn and M. Dincă, Conductive MOF Electrodes for Stable Supercapacitors with High Areal Capacitance, *Nat. Mater.*, 2017, **16**(2), 220–224; (*c*) K. Wada, K. Sakaushi, S. Sasaki and H. Nishihara, Multielectron-Transfer-Based Rechargeable Energy Storage of Two-Dimensional Coordination Frameworks with Non-Innocent Ligands, *Angew. Chem., Int. Ed.*, 2018, **57**(29), 8886–8890; (*d*) D. Feng, T. Lei, M. R. Lukatskaya, J. Park, Z. Huang, M. Lee, L. Shaw, S. Chen, A. A. Yakovenko, A. Kulkarni, *et al.*, Robust and Conductive Two-Dimensional Metal−Organic Frameworks with Exceptionally High Volumetric and Areal Capacitance, *Nat. Energy*, 2018, **3**(1), 30–36; (*e*) J. Park, M. Lee, D. Feng, Z. Huang, A. C. Hinckley, A. Yakovenko, X. Zou, Y. Cui and Z. Bao, Stabilization of Hexaaminobenzene in a 2D Conductive Metal–Organic Framework for High Power Sodium Storage, *J. Am. Chem. Soc.*, 2018, **140**(32), 10315–10323.

3 (*a*) Y. Sun, P. Sheng, C. Di, F. Jiao, W. Xu, D. Qiu and D. Zhu, Organic Thermoelectric Materials and Devices Based on p- and n-Type Poly(Metal 1,1,2,2-Ethenetetrathiolate)s, *Adv. Mater.*, 2012, **24**(7), 932–937; (*b*) F. Jiao, C. Di, Y. Sun, P. Sheng, W. Xu and D. Zhu, Inkjet-Printed Flexible Organic Thin-Film Thermoelectric Devices Based on p- and n-Type Poly(Metal 1,1,2,2-Ethenetetrathiolate)s/Polymer Composites through Ball-Milling, *Philos. Trans. R. Soc., A*, 2014, **372**, 8; (*c*) Y. Sun, L. Qiu, L. Tang, H. Geng, H. Wang, F. Zhang, D. Huang, W. Xu, P. Yue, Y. Guan, *et al.*, Flexible n-Type High-Performance Thermoelectric Thin Films of Poly(Nickel-Ethylenetetrathiolate) Prepared by an Electrochemical Method, *Adv. Mater.*, 2016, **28**(17), 3351–3358; (*d*) L. Sun, B. Liao, D. Sheberla, D. Kraemer, J. Zhou, E. A. Stach, D. Zakharov, V. Stavila, A. A. Talin, Y. Ge, *et al.*, A Microporous and Naturally Nanostructured Thermoelectric Metal–Organic Framework with Ultralow Thermal Conductivity, *Joule*, 2017, **1**(1), 168–177.

4 (*a*) Z. F. Wang, N. Su and F. Liu, Prediction of a Two-Dimensional Organic Topological Insulator, *Nano Lett.*, 2013, **13**(6), 2842–2845; (*b*) T. Kambe, R. Sakamoto, T. Kusamoto, T. Pal, N. Fukui, K. Hoshiko, T. Shimojima, Z. Wang, T. Hirahara, K. Ishizaka, *et al.*, Redox Control and High Conductivity of Nickel Bis(Dithiolene) Complex π-Nanosheet: A Potential Organic Two-Dimensional Topological Insulator, *J. Am. Chem. Soc.*, 2014, **136**(41), 14357–14360; (*c*) C. Chakravarty, B. Mandal and P. Sarkar, Bis(Dithiolene)-Based Metal–Organic Frameworks with Superior Electronic and Magnetic Properties: Spin Frustration to Spintronics and Gas Sensing, *J. Phys. Chem. C*, 2016, **120**(49), 28307–28319; (*d*) L. Liu, J. A. DeGayner, L. Sun, D. Z. Zee and T. D. Harris, Reversible Redox Switching of Magnetic Order and Electrical Conductivity in a 2D Manganese Benzoquinoid Framework, *Chem. Sci.*, 2019, **10**(17), 4652–4661.

5 (*a*) A. J. Clough, J. W. Yoo, M. H. Mecklenburg and S. C. Marinescu, Two-Dimensional Metal–Organic Surfaces for Efficient Hydrogen Evolution from Water, *J. Am. Chem. Soc.*, 2015, **137**(1), 118–121; (*b*) R. Dong, M. Pfeffermann, H. Liang, Z. Zheng, X. Zhu, J. Zhang and X. Feng, Large-Area, Free-Standing, Two-Dimensional Supramolecular Polymer Single-Layer Sheets for Highly Efficient Electrocatalytic Hydrogen Evolution, *Angew. Chem., Int. Ed.*, 2015, **54**(41), 12058–12063; (*c*) E. M. Miner, T. Fukushima, D. Sheberla, L. Sun, Y. Surendranath and M. Dincă, Electrochemical Oxygen Reduction Catalysed by Ni_3(Hexaiminotriphenylene)$_2$, *Nat. Commun.*, 2016, **7**(1), 10942; (*d*) X. Huang, H. Yao, Y. Cui, W. Hao, J. Zhu, W. Xu and D. Zhu, Conductive Copper Benzenehexathiol Coordination Polymer as a Hydrogen Evolution Catalyst, *ACS Appl. Mater. Interfaces*, 2017, **9**(46), 40752–40759; (*e*) E. M. Miner, L. Wang and M. Dincă, Modular O_2 Electroreduction Activity in Triphenylene-Based Metal–Organic Frameworks, *Chem. Sci.*, 2018, **9**(29), 6286–6291; (*f*) Z. Ji, C. Trickett, X. Pei and O. M. Yaghi, Linking Molybdenum–Sulfur Clusters for Electrocatalytic Hydrogen Evolution, *J. Am. Chem. Soc.*, 2018, **140**(42), 13618–13622.

6 (*a*) Q. Tang and Z. Zhou, Electronic Properties of π-Conjugated Nickel Bis(Dithiolene) Network and Its Addition Reactivity with Ethylene, *J. Phys. Chem. C*, 2013, **117**(27), 14125–14129; (*b*) M. G. Campbell, D. Sheberla, S. F. Liu, T. M. Swager and M. Dincă, Cu_3(Hexaiminotriphenylene)$_2$: An Electrically Conductive 2D Metal–Organic Framework for Chemiresistive Sensing, *Angew. Chem., Int. Ed.*, 2015, **54**(14), 4349–4352; (*c*) C. H. Hendon, A. J. Rieth, M. D. Korzynski and M. Dincă, Grand Challenges and Future Opportunities for Metal–Organic Frameworks, *ACS Cent. Sci.*, 2017, 554–563; (*d*) L. Liu, L. Li, J. A. DeGayner, P. H. Winegar, Y. Fang and T. D. Harris, Harnessing Structural Dynamics in a 2D Manganese–Benzoquinoid Framework To Dramatically Accelerate Metal Transport in Diffusion-Limited Metal Exchange Reactions, *J. Am. Chem. Soc.*, 2018, **140**(36), 11444–11453; (*e*) B. Hoppe, K. D. J. Hindricks, D. P. Warwas, H. A. Schulze, A. Mohmeyer, T. J. Pinkvos, S. Zailskas, M. R. Krey, C. Belke, S. König, *et al.*, Graphene-like Metal–Organic Frameworks: Morphology Control, Optimization of Thin Film Electrical Conductivity and Fast Sensing Applications, *CrystEngComm*, 2018, **20**(41), 6458–6471.

7 (*a*) L. E. Darago, M. L. Aubrey, C. J. Yu, M. I. Gonzalez and J. R. Long, Electronic Conductivity, Ferrimagnetic Ordering, and Reductive Insertion Mediated by Organic Mixed-Valence in a Ferric Semiquinoid Metal–Organic Framework, *J. Am. Chem. Soc.*, 2015, **137**(50), 15703–15711; (*b*) I.-R. Jeon, B. Negru, R. P. Van Duyne and T. D. Harris, A 2D Semiquinone Radical-Containing Microporous Magnet with Solvent-Induced Switching from $T_c = 26$ to 80 K, *J. Am. Chem. Soc.*, 2015, **137**(50), 15699–15702; (*c*) I.-R. Jeon, L. Sun, B. Negru, R. P. Van Duyne, M. Dincă and T. D. Harris, Solid-State Redox Switching of Magnetic Exchange and Electronic Conductivity in a Benzoquinoid-Bridged MnII Chain Compound, *J. Am. Chem. Soc.*, 2016, **138**(20), 6583–6590; (*d*) J. A. DeGayner, I.-R. Jeon, L. Sun, M. Dincă and T. D. Harris, 2D Conductive Iron-Quinoid Magnets Ordering up to $T_c = 105$ K *via* Heterogenous Redox Chemistry, *J. Am. Chem. Soc.*, 2017, **139**(11), 4175–4184; (*e*) M. E. Ziebel, L. E. Darago and J. R. Long, Control of Electronic Structure and Conductivity in Two-Dimensional Metal-Semiquinoid Frameworks of Titanium, Vanadium, and Chromium, *J. Am. Chem. Soc.*, 2018, **140**(8), 3040–3051; (*f*) J. A. DeGayner, K. Wang and T. D. Harris, A Ferric Semiquinoid Single-Chain Magnet *via* Thermally-Switchable Metal–Ligand Electron Transfer, *J. Am. Chem. Soc.*, 2018, **140**(21), 6550–6553.

8 (*a*) D. Sheberla, L. Sun, M. a Blood-Forsythe, S. Er, C. R. Wade, C. K. Brozek, A. Aspuru-Guzik and M. Dincă, High Electrical Conductivity in Ni_3(2,3,6,7,10,11-Hexaiminotriphenylene)$_2$, a Semiconducting Metal–Organic Graphene Analogue, *J. Am. Chem. Soc.*, 2014, **136**(25), 8859–8862; (*b*) J. H. Dou, L. Sun, Y. Ge, W. Li, C. H. Hendon, J. Li, S. Gul, J. Yano, E. A. Stach and M. Dincă, Signature of Metallic Behavior in the Metal–Organic Frameworks M_3(Hexaiminobenzene)$_2$ (M = Ni, Cu), *J. Am. Chem. Soc.*,

2017, **139**(39), 13608–13611; (*c*) L. S. Xie, L. Sun, R. Wan, S. S. Park, J. A. DeGayner, C. H. Hendon and M. Dincă, Tunable Mixed-Valence Doping toward Record Electrical Conductivity in a Three-Dimensional Metal–Organic Framework, *J. Am. Chem. Soc.*, 2018, **140**, 7411–7414; (*d*) J. G. Park, M. L. Aubrey, J. Oktawiec, K. Chakarawet, L. E. Darago, F. Grandjean, G. J. Long and J. R. Long, Charge Delocalization and Bulk Electronic Conductivity in the Mixed-Valence Metal–Organic Framework Fe(1,2,3-Triazolate)$_2$(BF$_4$)$_x$, *J. Am. Chem. Soc.*, 2018, **140**, 8526–8534.

9 (*a*) T. Kambe, R. Sakamoto, K. Hoshiko, K. Takada, M. Miyachi, J. H. Ryu, S. Sasaki, J. Kim, K. Nakazato, M. Takata, *et al.*, π-Conjugated Nickel Bis(Dithiolene) Complex Nanosheet, *J. Am. Chem. Soc.*, 2013, **135**(7), 2462–2465; (*b*) X. Huang, P. Sheng, Z. Tu, F. Zhang, J. Wang, H. Geng, Y. Zou, C. Di, Y. Yi, Y. Sun, *et al.*, A Two-Dimensional π–d Conjugated Coordination Polymer with Extremely High Electrical Conductivity and Ambipolar Transport Behaviour, *Nat. Commun.*, 2015, **6**(1), 7408; (*c*) H. Maeda, R. Sakamoto and H. Nishihara, Coordination Programming of Two-Dimensional Metal Complex Frameworks, *Langmuir*, 2016, **32**(11), 2527–2538; (*d*) X. Huang, H. Li, Z. Tu, L. Liu, X. Wu, J. Chen, Y. Liang, Y. Zou, Y. Yi, J. Sun, *et al.*, Highly Conducting Neutral Coordination Polymer with Infinite Two-Dimensional Silver–Sulfur Networks, *J. Am. Chem. Soc.*, 2018, **140**(45), 15153–15156; (*e*) R. Dong, P. Han, H. Arora, M. Ballabio, M. Karakus, Z. Zhang, C. Shekhar, P. Adler, P. S. Petkov, A. Erbe, *et al.*, High-Mobility Band-like Charge Transport in a Semiconducting Two-Dimensional Metal–Organic Framework, *Nat. Mater.*, 2018, **17**(11), 1027–1032; (*f*) Y. Cui, J. Yan, Z. Chen, J. Zhang, Y. Zou, Y. Sun, W. Xu and D. Zhu, [Cu$_3$(C$_6$Se$_6$)]$_n$: The First Highly Conductive 2D π–d Conjugated Coordination Polymer Based on Benzenehexaselenolate, *Adv. Sci.*, 2019, **6**(9), 1802235.

10 (*a*) L. Sun, T. Miyakai, S. Seki and M. Dincă, Mn$_2$(2,5-Disulfhydrylbenzene-1,4-Dicarboxylate): A Microporous Metal–Organic Framework with Infinite (–Mn–S–)$_\infty$ Chains and High Intrinsic Charge Mobility, *J. Am. Chem. Soc.*, 2013, **135**(22), 8185–8188; (*b*) L. Sun, M. G. Campbell and M. Dincă, Electrically Conductive Porous Metal-Organic Frameworks, *Angew. Chem., Int. Ed.*, 2016, **55**(11), 3566–3579; (*c*) N. E. Horwitz, J. Xie, A. S. Filatov, R. J. Papoular, W. E. Shepard, D. Z. Zee, M. P. Grahn, C. Gilder and J. S. Anderson, Redox-Active 1D Coordination Polymers of Iron–Sulfur Clusters, *J. Am. Chem. Soc.*, 2019, **141**(9), 3940–3951.

11 (*a*) J. L. Segura and N. Martin, New Concepts in Tetrathiafulvalene Chemistry, *Angew. Chem., Int. Ed.*, 2001, 1372–1409; (*b*) H. Wang, L. Cui, J. Xie, C. F. Leong, D. M. D'Alessandro and J. Zuo, Functional Coordination Polymers Based on Redox-Active Tetrathiafulvalene and Its Derivatives, *Coord. Chem. Rev.*, 2017, **345**, 342–361.

12 M. R. Bryce, Recent Progress on Conducting Organic Charge-Transfer Salts, *Chem. Soc. Rev.*, 1991, **20**(3), 355.

13 (*a*) T. C. Narayan, T. Miyakai, S. Seki and M. Dincă, High Charge Mobility in a Tetrathiafulvalene-Based Microporous Metal–Organic Framework, *J. Am. Chem. Soc.*, 2012, **134**(31), 12932–12935; (*b*) L. Sun, S. S. Park, D. Sheberla and M. Dincă, Measuring and Reporting Electrical Conductivity in Metal-Organic Frameworks: Cd$_2$(TTFTB) as a Case Study, *J. Am. Chem. Soc.*, 2016, **138**(44), 14772–14782; (*c*) L. S. Xie and M. Dincă, Novel Topology in Semiconducting Tetrathiafulvalene Lanthanide Metal-Organic Frameworks, *Isr. J. Chem.*, 2018, **58**(9–10), 1119–1122; (*d*) L. S. Xie, E. V. Alexandrov, G. Skorupskii, D. M. Proserpio and M. Dincă, Diverseπ–π Stacking Motifs Modulate Electrical Conductivity in Tetrathiafulvalene-Based Metal–Organic Frameworks, *Chem. Sci.*, 2019, **10**(37), 8558–8565.

14 (*a*) J. Su, S. Yuan, H.-Y. Wang, L. Huang, J.-Y. Ge, E. Joseph, J. Qin, T. Cagin, J.-L. Zuo and H.-C. Zhou, Redox-Switchable Breathing Behavior in Tetrathiafulvalene-Based Metal–Organic Frameworks, *Nat. Commun.*, 2017, **8**(1), 2008; (*b*) M. Souto, J. Romero, J. Calbo, I. J. Vitórica-Yrezábal, J. L. Zafra, J. Casado, E. Ortí, A. Walsh and G. Mínguez Espallargas, Breathing-Dependent Redox Activity in a Tetrathiafulvalene-Based Metal–Organic Framework, *J. Am. Chem. Soc.*, 2018, **140**(33), 10562–10569.

15 (*a*) H.-Y. Wang, J.-Y. Ge, C. Hua, C.-Q. Jiao, Y. Wu, C. F. Leong, D. M. D'Alessandro, T. Liu and J.-L. Zuo, Photo- and Electronically Switchable Spin-Crossover Iron(II) Metal-Organic Frameworks Based on a Tetrathiafulvalene Ligand, *Angew. Chem., Int. Ed.*, 2017, **56**(20), 5465–5470; (*b*) J. Su, T.-H. Hu, R. Murase, H.-Y. Wang, D. M. D'Alessandro, M. Kurmoo and J.-L. Zuo, Redox Activities of Metal–Organic Frameworks Incorporating Rare-Earth Metal Chains and Tetrathiafulvalene Linkers, *Inorg. Chem.*, 2019, **58**(6), 3698–3706.

16 (*a*) N. M. Rivera, E. M. Engler and R. R. Schumaker, Synthesis and Properties of Tetrathiafulvalene–Metal Bisdithiolene Macromolecules, *J. Chem. Soc., Chem. Commun.*, 1979, **4**, 184–185; (*b*) N. Yoshioka, H. Nishide, K. Inagaki, K. Inagaki and E. Tsuchida, Electrical Conductive and Magnetic Properties of Conjugated Tetrathiolate Nickel Polymers, *Polym. Bull.*, 1990, **23**(6), 631–636; (*c*) S. Dahm, W. Strunz, H. J. Keller and D. Schweitzer, Preparation and Physical Properties of Highly Conducting Metal (M = Ni, Co, Cu) Coordination Polymers, *Synth. Met.*, 1993, **55**(2–3), 884–889.

17 (*a*) R. D. McCullough and J. A. Belot, Toward New Magnetic, Electronic, and Optical Materials: Synthesis and Characterization of New Bimetallic Tetrathiafulvalene Tetrathiolate Building Blocks, *Chem. Mater.*, 1994, **6**(8), 1396–1403; (*b*) R. D. McCullough, J. A. Belot, A. L. Rheingold and G. P. A. Yap, Toward New Electronic, Magnetic, and Optical Materials: Structure and Properties of the First Homobimetallic Tetrathiafulvalene Tetrathiolate Building Block, *J. Am. Chem. Soc.*, 1995, **117**(39), 9913–9914; (*c*) R. D. McCullough, J. A. Belot, J. Seth, A. L. Rheingold, G. P. A. Yap and D. O. Cowan, Building Block Ligands for New Molecular Conductors: Homobimetallic Tetrathiafulvalene Tetrathiolates and

Metal Diselenolenes and Ditellurolenes, *J. Mater. Chem.*, 1995, **5**(10), 1581; (*d*) R. D. McCullough, J. Seth, J. A. Belot, S. A. Majetich and A. C. Carter, Novel Coordination Complexes of Tetrathiafulvalene Derivatives, *Synth. Met.*, 1993, **56**(1), 1989–1994.

18 (*a*) Y. Matsuo, M. Maruyama, S. S. Gayathri, T. Uchida, D. M. Guldi, H. Kishida, A. Nakamura and E. Nakamura, π-Conjugated Multidonor/Acceptor Arrays of Fullerene−Cobaltadithiolene−Tetrathiafulvalene: From Synthesis and Structure to Electronic Interactions, *J. Am. Chem. Soc.*, 2009, **131**, 12643–12649; (*b*) N. Bellec, A. Vacher, F. Barrière, Z. Xu, T. Roisnel and D. Lorcy, Interplay between Organic–Organometallic Electrophores within Bis(Cyclopentadienyl)Molybdenum Dithiolene Tetrathiafulvalene Complexes, *Inorg. Chem.*, 2015, **54**(10), 5013–5020.

19 N. Svenstrup, K. M. Rasmussen, T. K. Hansen and J. Becher, The Chemistry of TTFTT; 1: New Efficient Synthesis and Reactions of Tetrathiafulvalene-2,3,6,7-Tetrathiolate (TTFTT): An Important Building Block in TTF-Syntheses, *Synthesis*, 1994, 809–812.

20 (*a*) E. Cerrada, E. J. Fernandez, P. G. Jones, A. Laguna, M. Laguna and R. Terroba, Synthesis and Reactivity of Trinuclear Gold(III) Dithiolate Complexes. X-Ray Structure of $[Au(C_6F_5)(S_2C_6H_4)]_3$ and $[Au(C_6F_5)(S_2C_6H_4)(SC_6H_4SPPh_3)]$, *Organometallics*, 1995, **14**(12), 5537–5543; (*b*) S. M. S. V. Doidge-Harrison, J. T. S. Irvine, A. Khan, G. M. Spencer, J. L. Wardell and J. H. Aupers, Diorganotin 1,3-Dithiole-2-Thione-4,5-Dithiolate Compounds, R_2Sn(dmit): The Crystal Structure of MePhSn(dmit), *J. Organomet. Chem.*, 1996, **516**(1–2), 199–205; (*c*) J. H. Aupers, Z. H. Chohan, P. J. Cox, S. M. S. V. Doidge-Harrison, A. Howie, A. Khan, G. M. Spencer and J. L. Wardell, Syntheses and Structures of Diorgano(Halo-Orpseudohalo-)(1,3-Dithiole-2-Thione-4,5-Dithiolato)-Stannates (1-), [Q][R_2SnX(dmit)] (Q=Onium Cation; X=Halide or Pseudohalide), *Polyhedron*, 1998, **17**(25–26), 4475–4486; (*d*) E. Cerrada, S. Elipe, M. Laguna, F. Lahoz and A. Moreno, Dithiolate and Diselenolate Tin Complexes as Ligands Transfer Reagent towards Other Metals, *Synth. Met.*, 1999, **102**(1–3), 1759–1760; (*e*) C. J. Adams, N. Fey, M. Parfitt, S. J. A. Pope and J. A. Weinstein, Synthesis, Structures and Properties of a New Series of Platinum–Diimine–Dithiolate Complexes, *Dalton Trans.*, 2007, **39**, 4446; (*f*) K. S. Shin, Y. J. Jung, S. K. Lee, M. Fourmigué, F. Barrière, J. F. Bergamini and D. Y. Noh, Redox Bifunctionality in a Pt(II) Dithiolene Complex of a Tetrathiafulvalene Diphosphine Ligand, *J. Chem. Soc., Dalton Trans.*, 2008, **96**(43), 5869–5871; (*g*) R. Llusar, S. Triguero, V. Polo, C. Vicent, C. J. Gómez-García, O. Jeannin and M. Fourmigué, Trinuclear Mo_3S_7 Clusters Coordinated to Dithiolate or Diselenolate Ligands and Their Use in the Preparation of Magnetic Single Component Molecular Conductors, *Inorg. Chem.*, 2008, **47**(20), 9400–9409; (*h*) E. Cerrada, A. Moreno and M. Laguna, S,C- and S,S-Coupling *via* Dithiolate Transfer Reactions from Tin to Nickel Complexes, *Dalton Trans.*, 2009, **34**, 6825; (*i*) T. Ogawa, M. Sakamoto, H. Honda, T. Matsumoto, A. Kobayashi, M. Kato and H. Chang, Self-Association and Columnar Liquid Crystalline Phase of Cationic Alkyl-Substituted-Bipyridine Benzenedithiolato Gold(III) Complexes, *Dalton Trans.*, 2013, **42**(45), 15995.

21 (*a*) M. Nomura and M. Fourmigué, Dinuclear Cp* Cobalt Complexes of the 1,2,4,5-Benzenetetrathiolate Bischelating Ligand, *Inorg. Chem.*, 2008, **47**(4), 1301–1312; (*b*) K. Arumugam, M. C. Shaw, P. Chandrasekaran, D. Villagrán, T. G. Gray, J. T. Mague and J. P. Donahue, Synthesis, Structures, and Properties of 1,2,4,5-Benzenetetrathiolate Linked Group 10 Metal Complexes, *Inorg. Chem.*, 2009, **48**(22), 10591–10607.

22 (*a*) P. R. Ashton, V. Balzani, J. Becher, A. Credi, M. C. T. Fyfe, G. Mattersteig, S. Menzer, M. B. Nielsen, F. M. Raymo, J. F. Stoddart, *et al.*, A Three-Pole Supramolecular Switch, *J. Am. Chem. Soc.*, 1999, **121**(16), 3951–3957; (*b*) L. Wang, J.-P. Zhang and B. Zhang, Bis[Tetrakis(Methylsulfanyl) Tetrathiafulvalenium] Oxalate Dichloride, *Acta Crystallogr., Sect. E: Struct. Rep. Online*, 2005, **61**(6), 1674–1676; (*c*) J. Beck and A. Bof de Oliveira, On the Oxidation of Octamethylenetetrathiafulvalene by $CuBr_2$-Synthesis, Crystal Structure and Magnetic Properties of $[(OMTTF)_2Cu_4Br_{10}]$, *Z. Anorg. Allg. Chem.*, 2009, **635**(3), 445–449; (*d*) Y. Wang, S. Cui, B. Li, J. Zhang and Y. Zhang, Synthesis and Characterization of Monosubstituted TTF and Its Solvent Dependent Mono- and Dication Charge-Transfer Salts, *Cryst. Growth Des.*, 2009, **9**(9), 3855–3858; (*e*) G. Barin, M. Frasconi, S. M. Dyar, J. Iehl, O. Buyukcakir, A. A. Sarjeant, R. Carmieli, A. Coskun, M. R. Wasielewski and J. F. Stoddart, Redox-Controlled Selective Docking in a [2]Catenane Host, *J. Am. Chem. Soc.*, 2013, **135**(7), 2466–2469; (*f*) F. Gao, F. Zhu, X.-Y. Wang, Y. Xu, X. Wang and J. Zuo, Stabilizing Radical Cation and Dication of a Tetrathiafulvalene Derivative by a Weakly Coordinating Anion, *Inorg. Chem.*, 2014, **53**(10), 5321–5327.

23 (*a*) T. Mori and H. Inokuchi, Crystal and Electronic Structures of (BEDT-TTF)$AuCl_2AuCl_4$, *Chem. Lett.*, 1986, **15**(12), 2069–2072; (*b*) R. P. Shibaeva, R. M. Lobkovskaya, V. E. Korotkov, N. D. Kusch, É. B. Yagubskii and M. K. Makova, ET Cation-Radical Salts with Metal Complex Anions, *Synth. Met.*, 1988, **27**(1–2), 457–463; (*c*) K. A. Abboud, M. B. Clevenger, G. F. De Oliveira and D. R. Talham, Dication Salt of Bis(Ethylenedithio) Tetrathiafulvalene: Preparation and Crystal Structure of BEDT-TTF$(ClO_4)_2$, *J. Chem. Soc., Chem. Commun.*, 1993, **20**, 1560–1562; (*d*) T. Mori and H. Inokuchi, A BEDT-TTF Complex Including a Magnetic Anion, (BEDT-TTF)$_3(MnCl_4)_2$, *Bull. Chem. Soc. Jpn.*, 1988, **61**(2), 591–593; (*e*) M. Clemente-León, Hybrid Molecular Materials Based upon Organic π-Electron Donors and Inorganic Metal Complexes. Conducting Salts of Bis(Ethylenediseleno) Tetrathiafulvalene (BEST) with the Octahedral Anions Hexacyanoferrate(III) and Nitroprusside, *J. Solid State Chem.*, 2002, **168**(2), 616–625; (*f*) X. Xiao, H. Xu, W. Xu, D. Zhang and D. Zhu, Two Dication Salts of ET: Preparation and Crystal Structures of ET $[Fe^{II}(CN)_4(CO)_2]$,

Synth. Met., 2004, **144**(1), 51–53; (*g*) D. Belo, C. Rodrigues, I. C. Santos, S. Silva, T. Eusébio, E. B. Lopes, J. V. Rodrigues, M. J. Matos, M. Almeida, M. T. Duarte and R. T. Henriques, Synthesis, Crystal Structure and Magnetic Properties of Bis(3,4;3′,4′-Ethylenedithio)2,2′,5,5′-Tetrathiafulvalene-Bis(Cyanoimidodithiocarbonate) Aurate(III), (BEDT-TTF)[Au(CDC)$_2$], *Polyhedron*, 2006, **25**(5), 1209–1214; (*h*) H. Minemawari, T. Naito and T. Inabe, (ET)$_3$(Br$_3$)$_5$: A Metallic Conductor with an Unusually High Oxidation State of ET (ET = Bis(Ethylenedithio) Tetrathiafulvalene), *Chem. Lett.*, 2007, **36**(1), 74–75; (*i*) H. Minemawari, J. F. F. Jose, Y. Takahashi, T. Naito and T. Inabe, Structural Characteristics in a Stable Metallic ET Salt with Unusually High Oxidation State (ET: Bis(Ethylenedithio)Tetrathiafulvalene), *Bull. Chem. Soc. Jpn.*, 2012, **85**(3), 335–340; (*j*) M. Zecchini, J. R. Lopez, S. W. Allen, S. J. Coles, C. Wilson, H. Akutsu, L. Martin and J. D. Wallis, Exo-Methylene-BEDT-TTF and Alkene-Functionalised BEDT-TTF Derivatives: Synthesis and Radical Cation Salts, *RSC Adv.*, 2015, **5**(39), 31104–31112.

24 J.-C. Wu, S.-X. Liu, T. D. Keene, A. Neels, V. Mereacre, A. K. Powell and S. Decurtins, Coordination Chemistry of a π-Extended, Rigid and Redox-Active Tetrathiafulvalene-Fused Schiff-Base Ligand, *Inorg. Chem.*, 2008, **47**(8), 3452–3459.

25 (*a*) H. Spanggaard, J. Prehn, M. B. Nielsen, E. Levillain, M. Allain and J. Becher, Multiple-Bridged Bis-Tetrathiafulvalenes: New Synthetic Protocols and Spectroelectrochemical Investigations, *J. Am. Chem. Soc.*, 2000, **122**(39), 9486–9494; (*b*) J. Massue, N. Bellec, S. Chopin, E. Levillain, T. Roisnel, R. Clérac and D. Lorcy, Electroactive Ligands: The First Metal Complexes of Tetrathiafulvenyl–Acetylacetonate, *Inorg. Chem.*, 2005, **44**(24), 8740–8748; (*c*) M. B. Nielsen, C. Lomholt and J. Becher, Tetrathiafulvalenes as Building Blocks in Supramolecular Chemistry II, *Chem. Soc. Rev.*, 2000, **29**(3), 153–164.

26 M. Di Valentin, A. Bisol, G. Agostini, P. A. Liddell, G. Kodis, A. L. Moore, T. A. Moore, D. Gust and D. Carbonera, Photoinduced Long-Lived Charge Separation in a Tetrathiafulvalene–Porphyrin–Fullerene Triad Detected by Time-Resolved Electron Paramagnetic Resonance, *J. Phys. Chem. B*, 2005, **109**(30), 14401–14409.

27 D.-Y. Noh, E.-M. Seo, H.-J. Lee, H.-Y. Jang, M.-G. Choi, Y. H. Kim and J. Hong, Syntheses and Characterization of Heterobimetallic Complexes (dppf)Pt(Dithiolate) (dppf: (Diphenylphosphino)Ferrocene); X-Ray Crystal Structures of (dppf)PtL Where L=dmit, phdt and i-mnt, *Polyhedron*, 2001, **20**(15–16), 1939–1945.

28 K. Shin, Y. Han and D. Noh, Synthesis and Redox Property of Heterometallic (dppf)M(C$_8$H$_4$S$_8$) and (dppf)M(C$_6$S$_8$)M(dppf) (M = Pd and Pt, dppf = 1,1′-Bis(Diphenylphosphino) Ferrocene), *Bull. Korean Chem. Soc.*, 2003, **24**(2), 235–238.

29 V. Khodorkovsky, L. Shapiro, P. Krief, A. Shames, G. Mabon, A. Gorgues and M. Giffard, Do π-Dimers of Tetrathiafulvalene Cation Radicals Really Exist at Room Temperature?, *Chem. Commun.*, 2001, **1**(24), 2736–2737.

30 (*a*) H. Tanaka, A Three-Dimensional Synthetic Metallic Crystal Composed of Single-Component Molecules, *Science*, 2001, **291**, 285–287; (*b*) G. Matsubayashi, M. Nakano and H. Tamura, Structures and Properties of Assembled Oxidized Metal Complexes with C$_8$H$_4$S$_8$ and Related Sulfur-Rich Dithiolate Ligands, *Coord. Chem. Rev.*, 2002, **226**(1–2), 143–151; (*c*) A. Kobayashi, E. Fujiwara and H. Kobayashi, Single-Component Molecular Metals with Extended-TTF Dithiolate Ligands, *Chem. Rev.*, 2004, **104**(11), 5243–5264; (*d*) Y. Okano, B. Zhou, H. Tanaka and T. Adachi, High-Pressure (up to 10.7 GPa) Crystal Structure of Single-Component Molecular Metal [Au(TMDT)$_2$], *J. Am. Chem. Soc.*, 2009, **131**(20), 7169–7174; (*e*) B. Zhou, Y. Idobata, A. Kobayashi, H. Cui, R. Kato, R. Takagi, K. Miyagawa, K. Kanoda and H. Kobayashi, Single-Component Molecular Conductor [Cu(DMDT)$_2$] with Three-Dimensionally Arranged Magnetic Moments Exhibiting a Coupled Electric and Magnetic Transition, *J. Am. Chem. Soc.*, 2012, **134**(30), 12724–12731; (*f*) H. Cui, H. Kobayashi, S. Ishibashi, M. Sasa, F. Iwase, R. Kato and A. Kobayashi, A Single-Component Molecular Superconductor, *J. Am. Chem. Soc.*, 2014, **136**(21), 7619–7622; (*g*) B. Zhou, S. Ogura, Q. Z. Liu, H. Kasai, E. Nishibori and A. Kobayashi, A Single-Component Molecular Conductor with Metal–Metal Bonding, [Pd(hfdt)$_2$] (hfdt: Bis(Trifluoromethyl) Tetrathiafulvalenedithiolate), *Chem. Lett.*, 2016, **45**(3), 303–305; (*h*) L. Valade, D. de Caro, C. Faulmann and K. Jacob, TTF[Ni(Dmit)$_2$]$_2$: From Single-Crystals to Thin Layers, Nanowires, and Nanoparticles, *Coord. Chem. Rev.*, 2016, **308**, 433–444; (*i*) R. Silva, B. Vieira, M. Andrade, I. Santos, S. Rabaça, E. Lopes, J. Coutinho, L. Pereira, M. Almeida and D. Belo, Gold and Nickel Extended Thiophenic-TTF Bisdithiolene Complexes, *Molecules*, 2018, **23**(2), 424; (*j*) B. Zhou, S. Ishibashi, T. Ishii, T. Sekine, R. Takehara, K. Miyagawa, K. Kanoda, E. Nishibori and A. Kobayashi, Single-Component Molecular Conductor [Pt(dmdt)$_2$]—a Three-Dimensional Ambient-Pressure Molecular Dirac Electron System, *Chem. Commun.*, 2019, **55**(23), 3327–3330.

31 W. Lu, Y. Zhang, J. Dai, Q.-Y. Zhu, G.-Q. Bian and D.-Q. Zhang, A Radical-Radical and Metal–Metal Coupling Tetrathiafulvalene Derivative in Which Organic Radicals Directly Coordinate to Cu^{II} Ions, *Eur. J. Inorg. Chem.*, 2006, **2006**(8), 1629–1634.

32 (*a*) M. Nakata, H. Nakatsuji, M. Ehara, M. Fukuda, K. Nakata and K. Fujisawa, Variational Calculations of Fermion Second-Order Reduced Density Matrices by Semidefinite Programming Algorithm, *J. Chem. Phys.*, 2001, **114**, 8282–8292; (*b*) D. A. Mazziotti, Realization of Quantum Chemistry without Wave Functions through First-Order Semidefinite Programming, *Phys. Rev. Lett.*, 2004, **93**, 213001; (*c*) Variational Two-Electron Reduced-Density Matrix Theory, in *Reduced-Density-Matrix Mechanics: With Application to Many-Electron Atoms and Molecules*, ed. D. A. Mazziotti, John Wiley and Sons, Inc., Hoboken, NJ, 2007, pp 19−59; (*d*) G. Gidofalvi and D. A. Mazziotti, Active-Space Two-Electron Reduced-Density-Matrix Method: Complete Active-Space Calculations without

Diagonalization of the N-electron Hamiltonian, *J. Chem. Phys.*, 2008, **129**, 134108; (*e*) N. Shenvi and A. F. Izmaylov, Active-Space N-Representability Constraints for Variational Two-Particle Reduced Density Matrix Calculations, *Phys. Rev. Lett.*, 2010, **105**, 213003; (*f*) D. A. Mazziotti, Large-Scale Semidefinite Programming for Many-Electron Quantum Mechanics, *Phys. Rev. Lett.*, 2011, **106**, 083001; (*g*) D. A. Mazziotti, Two-Electron Reduced Density Matrix as the Basic Variable in Many-Electron Quantum Chemistry and Physics, *Chem. Rev.*, 2012, **112**, 244; (*h*) B. Verstichel, H. van Aggelen, W. Poelmans and D. Van Neck, Variational Two-Particle Density Matrix Calculation for the Hubbard Model Below Half Filling Using Spin-Adapted Lifting Conditions, *Phys. Rev. Lett.*, 2012, **108**, 213001; (*i*) J. Fosso-Tande, T.-S. Nguyen, G. Gidofalvi and A. E. DePrince III, Large-Scale Variational Two-Electron Reduced-Density-Matrix Driven Complete Active Space Self-Consistent Field Methods, *J. Chem. Theory Comput.*, 2016, **12**, 2260–2271; (*j*) D. A. Mazziotti, Enhanced Constraints for Accurate Lower Bounds on Many-Electron Quantum Energies from Variational Two Electron Reduced Density Matrix Theory, *Phys. Rev. Lett.*, 2016, **117**, 153001.

33 (*a*) A. W. Schlimgen, C. W. Heaps and D. A. Mazziotti, Entangled Electrons Foil Synthesis of Elusive Low-Valent Vanadium Oxo Complex, *J. Phys. Chem. Lett.*, 2016, **7**, 627–631; (*b*) A. W. Schlimgen and D. A. Mazziotti, Static and Dynamic Electron Correlation in the Ligand Noninnocent Oxidation of Nickel Dithiolates, *J. Phys. Chem. A*, 2017, **121**, 9377–9384; (*c*) A. R. McIsaac and D. A. Mazziotti, Ligand Non-innocence and Strong Correlation in Manganese Superoxide Dismutase Mimics, *Phys. Chem. Chem. Phys.*, 2017, **19**, 4656–4660; (*d*) J. M. Montgomery and D. A. Mazziotti, Strong Electron Correlation in Nitrogenase Cofactor, FeMoco, *J. Phys. Chem. A*, 2018, **122**, 4988–4996.

34 *Maple Quantum Chemistry Toolbox*, Maplesoft, a division of Waterloo Maple Inc., Waterloo, Ontario, 2019.

35 (*a*) J. Binkley, J. Pople and W. Hehre, Self-consistent Molecular Orbital Methods. 21 Small Split-valence Basis Sets for First-row Elements, *J. Am. Chem. Soc.*, 1980, **102**, 939–947; (*b*) M. Gordon, J. Binkley, J. Pople, W. Pietro and W. Hehre, Self Consistent Molecular Orbital Methods. 22 Small Split-valence Basis Sets for Second-row Elements, *J. Am. Chem. Soc.*, 1982, **104**, 2797–2803; (*c*) K. Dobbs and W. Hehre, Molecular Orbital Theory of the Properties of Inorganic and Organometallic Compounds. 5 Extended Basis Sets for First-row Transition Metals, *J. Comput. Chem.*, 1987, **8**, 861–879; (*d*) K. Dobbs and W. Hehre, Molecular Orbital Theory of the Properties of Inorganic and Organometallic Compounds. 6 Extended Basis Sets for Second-row Transition Metals, *J. Comput. Chem.*, 1987, **8**, 880–893.

36 S. Alvarez, R. Vicente and R. Hoffmann, Dimerization and Stacking in Transition-Metal Bisdithiolenes and Tetrathiolates, *J. Am. Chem. Soc.*, 1985, **107**(22), 6253–6277.

37 T. Vogt, C. Faulmann, R. Soules, P. Lecante, A. Mosset, P. Castan, P. Cassoux and J. Galy, A LAXS (Large Angle X-Ray Scattering) and EXAFS (Extended X-Ray Absorption Fine Structure) Investigation of Conductive Amorphous Nickel Tetrathiolato Polymers, *J. Am. Chem. Soc.*, 1988, **110**(6), 1833–1840.